Vortex Modes in Southern Lake Michigan[1]

JAMES H. SAYLOR AND JOSEPH C. K. HUANG

Great Lakes Environmental Research Laboratory, NOAA, Ann Arbor, MI 48104

ROBERT O. REID

Department of Oceanography, Texas A&M University, College Station 77843

(Manuscript received 16 October 1979, in final form 1 August 1980)

ABSTRACT

Current velocities and water temperatures were observed in southern Lake Michigan with an array of AMF vector-averaging current meters during late spring, summer and fall 1976. Analyses of the recorded current data have revealed that persistent oscillations of nearly 4 days in period were at least as energetic as inertial oscillations in the kinetic energy spectra and current hodographs. The 4-day oscillations were present at all stations, including a very clear signal at stations near the center of the lake basin. This lake-wide oscillation was present during both stratified and unstratified seasons and current vectors rotated cyclonically near the center of the lake and anticyclonically elsewhere. The observed rotational oscillations closely fit the characteristics of barotropic second-class motions of a basin with variable depth first described by Lamb (1932). While such topographic vortex modes are of the same class as low-frequency shelf waves, their kinematic properties and natural period are governed by the lake shape as well as the bathymetry. Moreover, the gravest mode is unique among these waves in having nonzero velocity at the lake center. The present observations give clear evidence for the existence of the gravest mode of such oscillations in southern Lake Michigan.

1. Introduction

Between May and November 1976, an array of current meters was maintained in the southern basin of Lake Michigan (Fig. 1). The array was placed to study the properties of near-inertial period currents associated with internal Poincaré waves and to detect the propagation of either internal Kelvin waves or barotropic shelf waves along Lake Michigan's east coast. Also, the measurements provided estimates of water volume transport into and out of the southern part of the lake basin across the transverse cross section and information concerning the spatial distributions of these transports.

As part of an investigation of the propagation of long, coastally trapped waves, current and water temperature data from four, perpendicular-to-shore cross sections were first low-pass filtered to remove the energetic near-inertial period oscillations. Visual inspection of the remaining longer period motions in the coastal water of southern Lake Michigan revealed a remarkably persistent oscillation with a period of approximately 4 days. Spectral analyses of all current recordings revealed that the wave motions were not confined to the nearshore region, but in fact dominated the low-frequency end of the spectra at all offshore stations as well. The wave forms are therefore quite different from the internal Kelvin waves that were first reported in southern Lake Michigan by Mortimer (1963) and later detected along the southern coast of Lake Ontario by Csanady and Scott (1974).

The purpose of this paper is to report the low-frequency oscillatory wave phenomena observed in southern Lake Michigan and to explain dynamically the mechanisms producing the resultant current pattern. We found that the oscillations in the offshore waters of southern Lake Michigan fit very closely the characteristics of the classic second-class motions of a shallow liquid (vortex modes) studied analytically by Lamb (1932) for a circular basin and by Ball (1965) for an elliptic basin. In the better known example of second-class motions, the gradient of potential vorticity necessary for the oscillations (Rossby waves) is provided by the latitudinal variation of the vertical component of the earth's vorticity. In lakes, as on the continental shelf, the variation in potential vorticity is provided by the variation of the local depth, essentially controlled by the topography. As in many such problems we might expect that the gravest vortex modes (lowest wavenumber) would be dominant and, indeed, we will show herein the similarity of the Lake Michigan observations to the simplest analytical examples, which provide estimates of period and kinematical properties for comparison.

[1] GLERL Contribution No. 193.

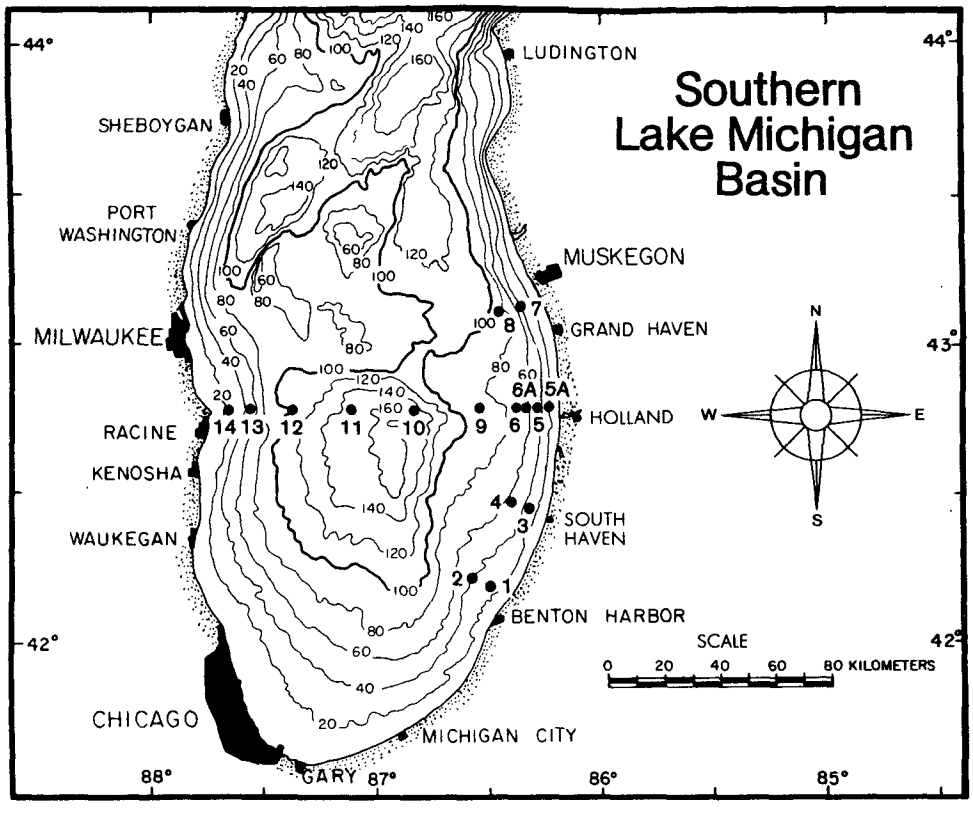

FIG. 1. Location map showing the bathymetry of southern Lake Michigan and the positions of the 16 current meter moorings.

Rotational modes in lakes have been discussed in theoretical normal mode calculations [cf. Hamblin (1972) and Rao and Schwab (1976)] and in analytical studies of circulations in rotating basins (Birchfield and Hickie, 1977). They also emerged as potential contributors to lake circulation in the numerical model results of Simons (1974). However, existing studies relating the theoretical and observational aspects of rotational modes in lakes are somewhat lacking in respect to identification of their lake-wide character. The nearshore properties of the rotational modes are similar to those of the topographic shelf wave model utilized by Csanady (1976) in analyses of Lake Ontario coastal currents. Here we will emphasize the offshore properties which make these oscillations unique, particularly for the gravest mode. To our knowledge, this variety of low-frequency wave phenomena has not been directly detected previously in current recordings from the interior of the lake basins.

In the following section of the paper the measurements are described. Observational results are presented in Section 3. Mean flow patterns and their seasonal variations are discussed first. The oscillatory nature of the low-pass filtered currents are then clearly demonstrated by velocity component plots and current hodographs. Currents in the center of the lake basin reveal cyclonic rotation, while currents recorded closer to shore reveal anticyclonic rotation. Spectral analyses show two distinct peaks, one at the local inertial period and one at nearly 4 days. In Section 4, the observed rotational oscillations are related to predictions from simple developments given here and by Ball (1965), which are generalizations of the circular paraboloidal basin model first treated by Lamb (1932). The sensitivity of the vortex modes to the approximation of bottom topography is investigated and we conclude that the gravest mode best fits the observations for a conical parameterization.

2. Description of measurements

The experimental plan was originally designed to investigate two physical processes in southern Lake Michigan (Fig. 1). Near-inertial period currents have close association with long-wavelength internal Poincaré waves in the Great Lakes during seasons of strong density stratification (Mortimer, 1963), and the transverse cross section of the lake was instrumented to study the cross-channel properties of these waves. Coastally trapped shelf waves and internal Kelvin waves propagate relatively slowly along the lake coasts and the perpendicular-

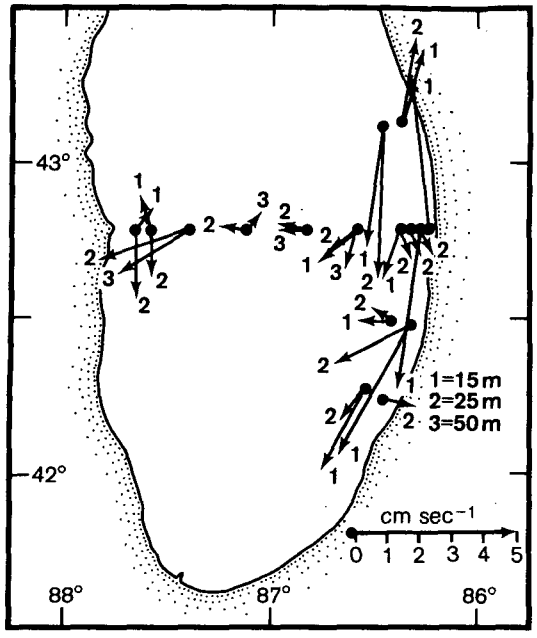

FIG. 2. Vector-averaged current observed in southern Lake Michigan for the interval 20 May–30 June 1976.

to-shore coastal cross sections were planned as antennas to detect their signals. For conditions representative of typical summer stratification in Lake Michigan, internal Kelvin waves would have phase speeds of ~ 0.5 m s^{-1}. With the coastal cross sections spaced at just over 30 km intervals along the east shore of the lake, northward propagating Kelvin waves would pass through the sections at intervals slightly longer than two-thirds of a day.

Currents and water temperatures were measured with AMF vector-averaging current meters recording at 15 min intervals. The meters were suspended on a taut line below streamlined subsurface floats located just above the uppermost instrument on each mooring. All of the 16 moorings had current meters at 12.5 and 25 m beneath the water surface. Moorings 9–12, placed in deep water near the center of the basin, also had a current meter at 50 m depth. An acoustical release was placed in each string just above the mooring's anchor. A back-up recovery system was provided by stretching a ground line of 200 m of polypropylene rope between the mooring's anchor and a secondary anchor. The current meters were deployed from the Environmental Protection Agency (EPA) R.V. *Roger R. Simons* in May 1976 and all except those on mooring 10 were recovered in November of the same year. Because of the failure of the acoustical release on mooring 10, it was not recovered until June 1977. In retrospect, this was fortunate because it provided three current meter records continuous through the winter for comparison with results during the ice-free season.

Accuracy of the temperature measurements is within 0.1°C. Velocity measurement characteristics of the Savonious rotor and of the AMF vector-averaging current meter are relatively well known (e.g., see Beardsley *et al.*, 1977). It is sufficient to note here that the subsurface floats supporting each mooring were placed just slightly deeper than 10 m, deep enough to be below any significant, long-lasting surface wave influences in the moderate wave climate in Lake Michigan during the summer and early fall. Another factor influencing the measurements was the omnipresent and continuous near-inertial period currents, which had speeds large enough that near-zero velocities were almost never recorded. This fact minimizes concern with the threshold speeds of the Savonious rotors. It also places the majority of speed recordings in the range of 10 to 50 cm s^{-1}, a range in which the rotor calibrations are quite linear and uniform from instrument to instrument.

3. Results

a. Mean flows

Although the mooring array was not configured to determine in any detail the circulation of the southern basin of Lake Michigan, it is pertinent to some later considerations to look at the mean flows existing during the measurement period. We have divided the period into three separate intervals for discussion; the intervals were determined by the structure of the lake's temperature (density) field.

From the time of current meter deployment until

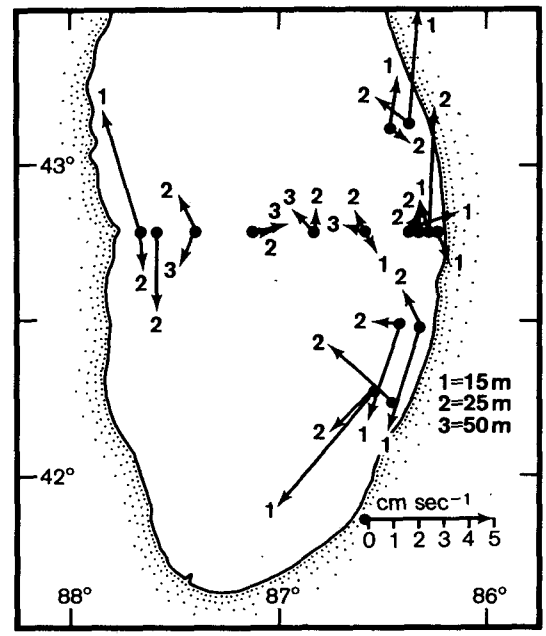

FIG. 3. As in Fig. 2 except for the interval 1 July–31 August 1976.

the end of June, the surface waters of the lake were slowly warming, but development of a well-defined thermocline across the entire basin had not yet occurred. Warming of the surface waters proceeded from the coast lakeward, with warm water initially confined to a narrow coastal strip encircling a core of cold water in the center of the basin. Lakeward expansion and thickening of the wedges of coastal warm water concluded near the end of June with development of a shallow thermocline across the lake. Winds during the period were generally light, caused in part by the stable stratification in warm air masses over the cold water surface. Vector resultant current flows observed during this period are shown in Fig. 2. Along the east coast, currents were directed southward, except very near the coast at stations 5A and 7 (Fig. 1), where a northward countercurrent was present. Velocities were small, only a few centimeters per second, and although the flow pattern is generally similar to the thermally driven currents predicted by Huang (1972) and others across the temperature front during the spring "thermal bar" season, the offshore southward velocities were too large to result from simply thermal considerations. At the western end of the cross section, currents were weakly northward at 12.5 m and southward at deeper levels; the pattern does not conform with thermal expectations. At the levels measured, currents in the center of the basin were weakly westward and southwestward. Return northward flow must have occurred at deeper levels in the center of the basin.

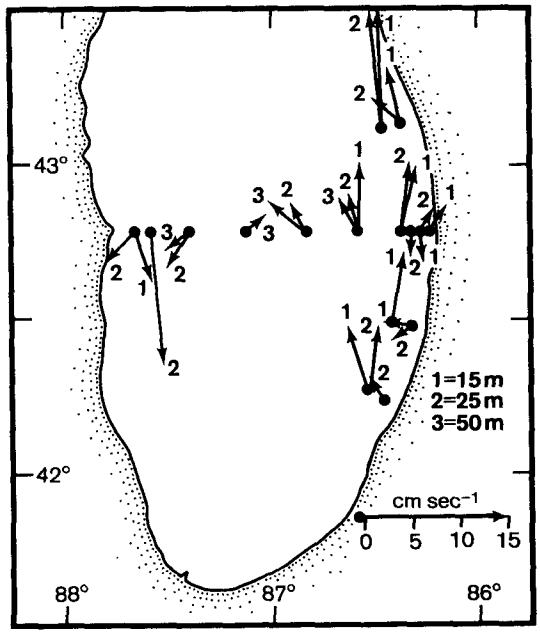

FIG. 4. As in Fig. 2 except for the interval 1 September–31 October 1976.

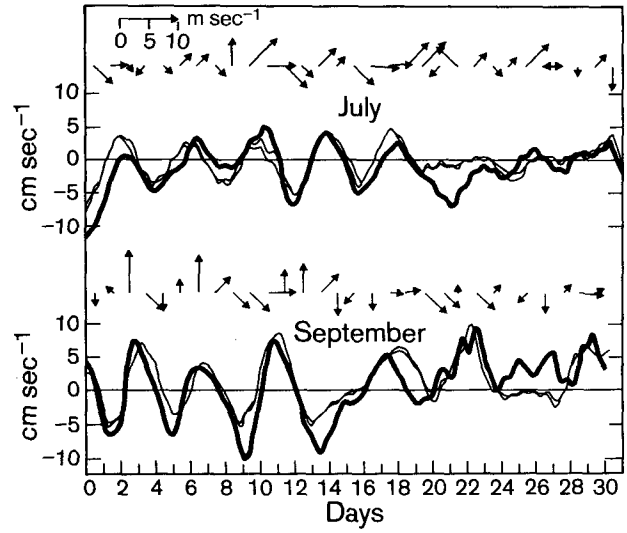

FIG. 5. The northward velocity component at the three levels of measurement at station 9 for July and September 1976. The thick line shows currents at 12.5 m; thin lines are from 25 and 50 m depth. Daily vector resultant winds recorded at the Muskegon airport are shown above each velocity trace.

The months of July and August were characterized by a shallow thermocline spread across the entire basin; its depth was generally less than 25 m. The surface layer was thicker near both coasts, but only during occasional downwellings did the thermocline penetrate the 25 m level. Light to moderate winds dominated, and alternate northerly and southerly wind pulses drove currents in either direction along the coasts. The resultant current flows during this period are shown in Fig. 3. Within the upper layer, currents at 12.5 m exhibited a divergent pattern from a stagnation point located somewhere offshore from Holland, Michigan. To the north of this area, flow was northward in the surface layer, and to the south, it was southward. This observed feature is in agreement with Monahan and Pilgram's (1975) suggestion that a local accumulation originates from an eastward surface drift constrained by the coastal configuration. As will be shown later, however, it is possible that the divergent flow near the coast results partially from the rotational waves propagating cyclonically in the basin. At the 25 m level, below the thermocline, the coastal flow pattern was weak but cyclonic. In the center of the basin, mean flows were slight at the levels of measurement and the flow pattern disorganized.

During September, intensifying fall storms quickly thickened the surface layer, pushing the thermocline below 25 m depth. Winds prevailed from the westerly quadrants. The pattern of mean flows observed during September and October are shown in Fig. 4. Flow across the lake cross section was strongly cyclonic at all levels, with northward di-

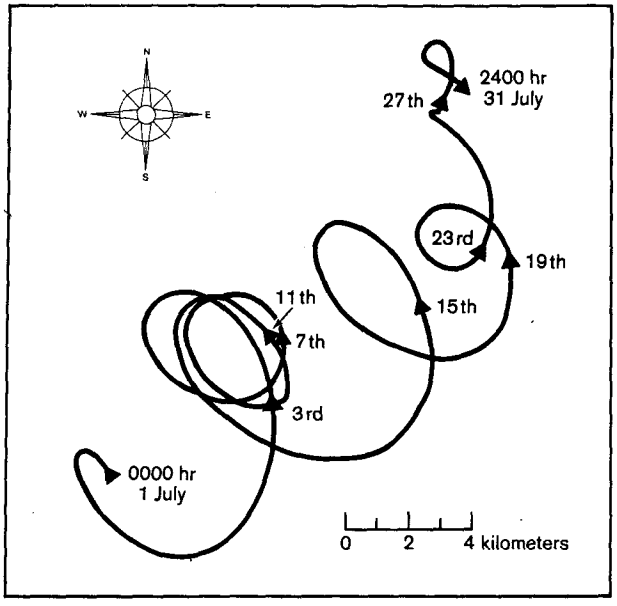

FIG. 6. Hodograph of hourly averaged, low-pass filtered current velocities from the 32 m depth current meter at station 11 for the month of July 1976.

rected currents dominating the eastern half of the lake basin except very near the shore. The cyclonic pattern intensified through the first half of November, at which time the current meters were removed. At that time, horizontal gradients of temperature had virtually disappeared and the mixed surface layer had penetrated below 50 m. The observed strong cyclonic flow is later hypothesized to influence the period of low-frequency waves through the mechanism of Doppler shift.

b. Oscillatory currents

To examine the nearshore current recordings for evidence of coastally trapped wave-like motions, we separately low-pass filtered the north and south velocity components to remove the energetic near-inertial period components. Inspection of the remaining low-frequency signals revealed an unusually persistent oscillation of nearly 4 days period at all coastal stations. Inspection of the offshore stations showed an even more regular wavelike structure closely tuned to the nearshore oscillations. Fig. 5 displays the northerly velocity observed at all three levels of measurement at station 9 during July and September 1976. Also shown in the figure are daily resultant wind vectors from Muskegon, Michigan. It is obvious that the motions were dominantly barotropic as the current was nearly in phase and of like amplitude at each level and the thermocline was between the upper and lower current meters. For example, the monthly mean temperature was 13.8°C at 12.5 m, 5.4°C at 25 m and 4.5°C at 50 m during September. The same barotropic nature was observed at all stations when the 4-day period was well developed.

Because the oscillation was so prominent in both the north and the east velocity components at all offshore stations, it appeared likely to be present in current hodographs. Fig. 6 shows the hodograph of hourly averaged, low-pass filtered currents from station 11 at the 32 m level for the month of July. (Because the ground line was fouled into the lower section of the mooring on deployment, the planned depths at this station were exceeded by 7 m.) The hodograph clearly reveals the oscillatory wave motion with a period of about 4 days, the rotation of the current vector being in a cyclonic direction for this station, which is in the center of the lake basin. In fact, in addition to a modest northeastward mean flow evident from 1 to 3 July and from 13 July to the end of the month, the hodograph presents an almost pure rotational mode of about 4-day period dominating central Lake Michigan. It is present in its purest form in the deeper current recordings near the center of the basin, where away from the coastal boundaries the north and east components are of similar magnitude and where direct wind forcing is minimized.

c. Spectra of current flow

Kinetic energy spectra of the east (u) and the north (v) velocity components are presented sepa-

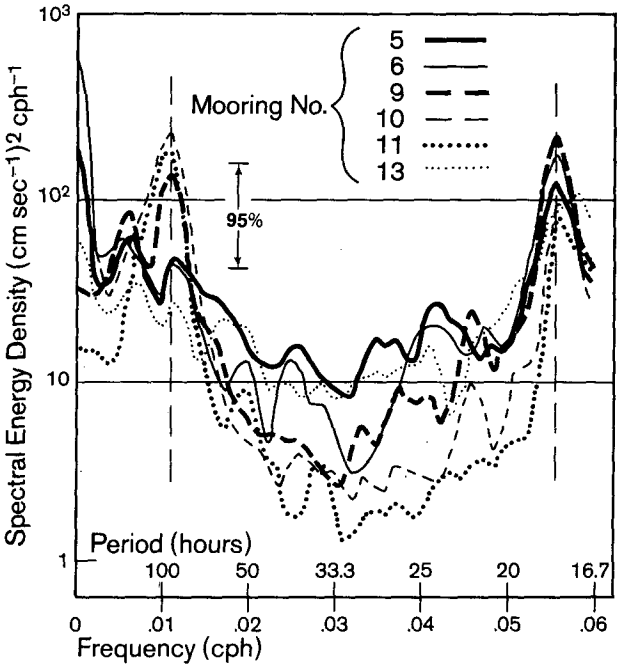

FIG. 7. Kinetic energy spectra of the eastward velocity component (u) recorded at the 25 m level at six stations in southern Lake Michigan. Vertical lines are drawn to accentuate the two conspicuous energy peaks at near-inertial and near 4-day periods.

rately in Figs. 7 and 8. The spectra and cross spectra were computed by use of the fast Fourier transform method. All were computed from multiple, overlapping, unfiltered data subsets of 256 values of 8 h averaged data, regularly spaced through the analysis interval, which were first transformed and then ensemble-averaged and smoothed by Hanning. The spectra of both the u and v components show a remarkably strong and distinct energy peak at a period of just less than 4 days. (The peak occurs at a period of 90 h, but the adjacent spectral estimates are made at periods of 93 and 85 h and the mode lies somewhere between these two values.) This spectral peak is pronounced at all stations in the v component (Fig. 8) and is suppressed in amplitude in the u component near the coasts as one would expect. We note that in the v component near the coasts the energy level is higher at all lower frequencies because of the presence there of quasi-geostrophic, shore-parallel currents that develop in all of the Great Lakes in response to long-lived wind stress impulses. Offshore, the energy levels at lower frequencies are much reduced and the spectra are dominated by two wave frequencies: the near-inertial period response and the 4-day response. This is shown clearly in Fig. 9, which illustrates the coherence and phase relationships between the u and v components for one current meter on mooring 11 and shows the highly correlated signals centered about the two frequencies.

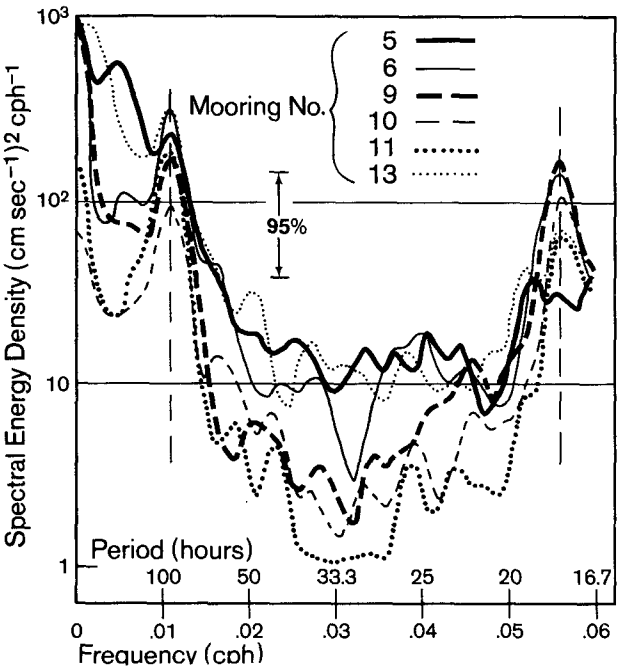

FIG. 8. As in Fig. 7 except for the northward velocity component (v).

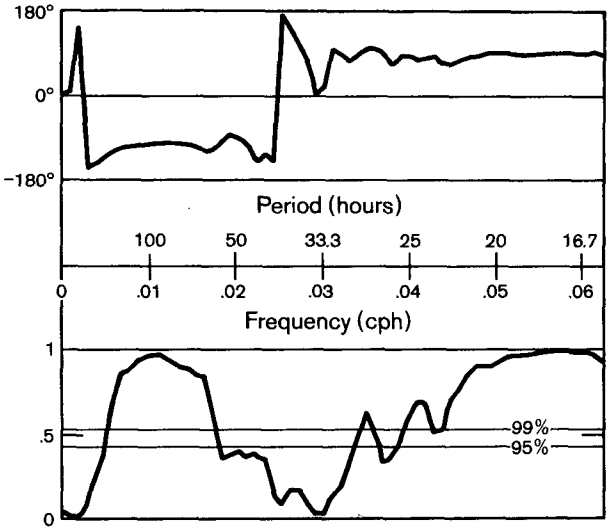

FIG. 9. Coherence (lower) and phase between the east and north velocities at the 32 m level from station 11. Two broad areas of high coherence highlight the cyclonic rotating 4-day oscillation and the anti-cyclonic near-inertial oscillation.

Cross-spectral estimates of coherence and phase are given for several station pairs in Table 1. The u component is very nearly in phase at all stations on the lake cross section. The v component at stations 10 and 11, in the center of the lake basin, is very nearly 180° out of phase with all of the stations closer to shore on the transect. Along the east coast of Lake Michigan the phase relationships show that the oscillation propagates northward, establishing a cyclonic wave rotation around the basin.

We calculated the average observed amplitude of the current oscillations across the lake basin for an episode of dominant rotational wave activity

TABLE 1. Cross-spectral estimates of coherence and phase at the frequency of 0.011 cycles per hour for selected station pairs that reveal 1) northward propagation of the wave along the east coast, 2) out-of-phase northward velocity components in the center of Lake Michigan, and 3) in-phase eastward velocity components across the entire basin.

Station pair	Coherence	Phase
Northward velocity component		
2 and 3	0.78	2 leads 3 by 38°
1) 2 and 6	0.88	2 leads 6 by 74°
2 and 8	0.69	2 leads 8 by 135°
6 and 9	0.94	6 lags 9 by 10°
2) 6 and 11	0.88	6 lags 11 by 172°
6 and 12	0.91	6 lags 12 by 28°
Eastward velocity component		
6 and 9	0.86	6 lags 9 by 5°
3) 6 and 11	0.79	6 leads 10 by 26°
6 and 13	0.93	6 lags 13 by 16°

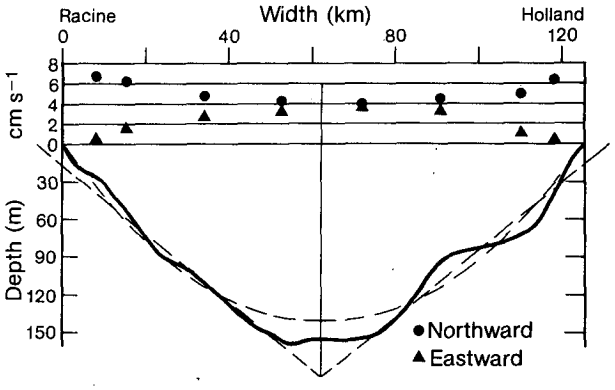

FIG. 10. Average amplitudes of the north and east velocity components for rotational oscillations on the southern Lake Michigan cross section during an episode of wave excitation, 1–15 July 1976. Basin approximations as a paraboloid or as an inverted cone that are referred to later are also shown.

during the first half of July (Fig. 10). The amplitude of the in-phase eastward component is largest in the center of the basin and decreases monotonically toward both coasts. The amplitude of the northward component is nearly uniform across much of the basin but increases along the coasts as rotational wave theory implies. It must be kept in mind, though, that the northward components of the rotational wave-induced currents at the two center stations are just counter to the alongshore currents on both coasts.

Rotary spectra (Gonella, 1972) were also computed at each station; several examples are shown in Fig. 11. As is well known, the near-inertial period motions are associated with clockwise rotation of the current vector. The 4-day period motions are also clockwise rotations at all stations except 10 and 11 in the center of the lake; there they are counterclockwise rotations. Also included in Fig. 11 are spectra from mooring 10 for data collected during winter 1976–77. They show that the vortex mode is as dominant in winter (when there is little density stratification) as in summer, further verifying the barotropic nature of the 4-day oscillation.

Excitation of the 4-day oscillation must be related to meteorological forcing; in particular, wave initiation appears to be responsive to short-lived impulses of southward-directed wind stress along the major axis of the lake (Fig. 5). These impulses drive currents southward with the wind along both lake coasts; northward return flow occurs near the center of the basin. Following relaxation of the southward wind stress, we observed in almost every instance a resurgent northward flow along both coasts, reaching its maximum intensity along the east coast of the lake with the northward propagating wave crest. This resurgence occurred irrespective of the wind history following the northerly storm. When the timing of the southward-directed impulses approached almost 4-day intervals, the amplitude of the oscillatory velocity components grew in almost resonant fashion.

4. Free vortex modes

Based on the evidence presented in Section 3 we confine our attention to possible barotropic free modes of the lake. All of the barotropic gravity modes, including any Kelvin-like modes, are of frequency ω greater than the Coriolis parameter f as long as the horizontal scale of the basin (L) is less than the barotropic radius of deformation $R = (gH)^{1/2}/f$, where H is the maximum depth and g is gravity (Lamb, 1932, ¶211). Since $L/R \ll 1$ for the Great Lakes, this rules out any gravity type mode as a candidate for the observed subinertial barotropic mode. However, if the basin is of variable depth with greatest depth in the central regions, then subinertial ($\omega < f$), cyclonically propagating, vortex modes can exist for *any* value of L/R (Lamb, 1932, ¶212). Moreover, for the gravest modes—those with the least number of circulational cells—the energy is not confined to the coastal region as in a large basin ($L \gg R$) with continental shelf-type bathymetry.

Both gravity modes and vortex modes can be analyzed in terms of the primitive depth-integrated equations of motion, as in Lamb's (1932) analysis for a closed basin and Reid's (1958) analysis for a continental shelf of constant slope. However, it is

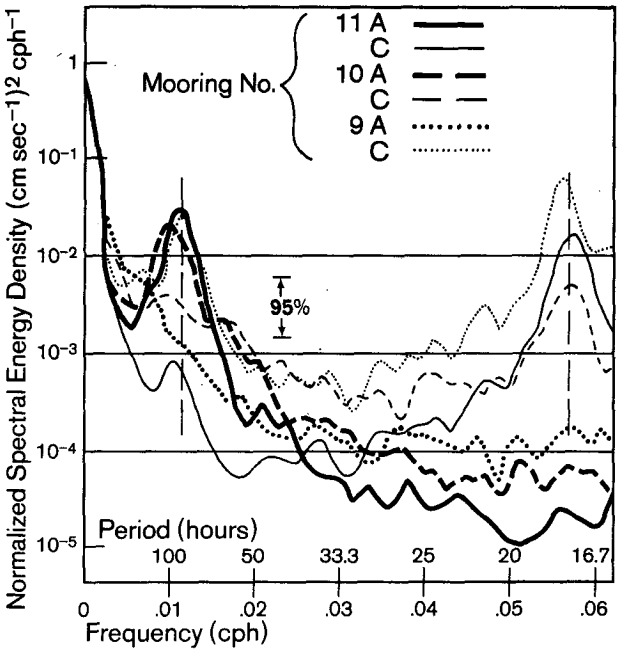

FIG. 11. Rotary spectra showing the clockwise (C) and anticlockwise (A) components of the current velocities recorded at stations 9, 10 and 11. The spectra for station 10 are from the winter of 1976–77.

now well known that the dynamics of the vortex modes for an inviscid fluid is best understood in terms of conservation of absolute potential vorticity, $(f + \xi)/h$, following a fluid column, where h is the local depth of the column and ξ its vertical component of relative vorticity. One can filter the gravity modes from consideration by employing a rigid-lid approximation in which the flow and the vorticity can be expressed in terms of a volume transport streamfunction ψ. The latter approximation is particularly justified for basins which satisfy the constraint $L/R \ll 1$ (Ball, 1965). The linearized vorticity equation for free disturbances then takes the form

$$\frac{\partial}{\partial t} \nabla \cdot (h^{-1} \nabla \psi) + J(\psi, f/h) = 0, \tag{1}$$

where J is the Jacobian operator. Solutions for ψ are subject to the condition that ψ be constant (say, zero) around the closed boundary of the basin. In small basins the dominant contribution to the "restoring" term J is via vortex stretching (h variations) rather than variation of f as in Rossby wave dynamics. Hereafter, we will consider f a constant for the basin.

One possible solution of (1) is a steady ($\omega = 0$) circulation mode in which $\psi = F(h)$; this will satisfy the boundary condition if h is constant around the boundary (e.g., zero). In order to investigate other vortex modes with nonzero frequency, one obviously must be more specific in regard to the structure of h. Simple separable solutions are possible only if h varies with one of two horizontal coordinates. As a rough approximation of southern Lake Michigan, which contains a well-defined deep region south of 43°N (Fig. 1), we consider this as a circular basin with radial depth profile

$$h = H[1 - (r/b)^m], \tag{2}$$

where H is the maximum depth and b the equivalent basin radius. The exponent m is 2 for a paraboloidal basin parameterization and is 1 for a conical basin (Fig. 10). We could employ Lamb's (1932) results directly for the paraboloidal case; however, it is instructive to see if (1) can reproduce his results for the limiting case of $b/R \ll 1$ (his analysis employed a free surface). It is also of interest to examine the sensitivity of the solutions to the profile shape parameter m. For periodic solutions in time (t) and azimuth (ϕ),

$$\psi = \psi_0(r) \cos(\omega t - k\phi), \tag{3}$$

and (1) reduces to

$$\frac{h}{r}\frac{d}{dr}\left(rh^{-1}\frac{d\psi_0}{dr}\right) - \left(\frac{k^2}{r^2} + \frac{f}{\omega}\frac{k}{hr}\frac{dh}{dr}\right)\psi_0 = 0, \tag{4}$$

where k is an integer characterizing the azmuthal mode. We are primarily concerned with possible modes which have no nodal circles of ψ except at $r = b$. It can be verified that a solution of this type is simply

$$\psi_0 = A(r/b)^k h^2, \tag{5}$$

where A is an arbitrary constant with dimensions of velocity. This solution satisfies (4) provided that

$$\omega = \frac{k}{(2m + 3k)} f. \tag{6}$$

The associated azmuthal and radial velocity components are

$$\left.\begin{aligned} V_\phi &= \frac{1}{h}\frac{\partial \psi}{\partial r} \\ &= \frac{AH}{b}\left[k - (2m + k)\left(\frac{r}{b}\right)^m\right]\left(\frac{r}{b}\right)^{k-1} \\ &\qquad \times \cos(\omega t - k\phi) \\ V_r &= -\frac{1}{rh}\frac{\partial \psi}{\partial \phi} \\ &= \frac{-AH}{b} k\left[1 - \left(\frac{r}{b}\right)^m\right]\left(\frac{r}{b}\right)^{k-1} \\ &\qquad \times \sin(\omega t - k\phi) \end{aligned}\right\}. \tag{7}$$

For $\phi = 0$, V_r and V_ϕ are equivalent, respectively, to x and y components for any r, including $r = 0$. The current hodographs are elliptical with counterclockwise rotation for $0 < r < r_c$ and clockwise rotation for $r_c < r < b$, where

$$r_c = b[k/(2m + k)]^{1/m}. \tag{8}$$

At $r = 0$ the current vanishes *except* for the mode $k = 1$, for which a circular hodograph exists.

For $k = 0$ we have a special case of a steady single-cell circulation mode. For $k = 1$ the streamfunction consists of two circulational cells of opposite sense, separated by a nodal diameter which has a cyclonic precession, of angular velocity

$$\omega = \frac{1}{(2m + 3)} f. \tag{9}$$

For the paraboloidal basin $\omega = f/7$, which is consistent with Lamb's analysis for the same mode in the limit of small b/R. At latitude 43° this yields a period of 123 h, which is significantly larger than the approximate period of 90 h found from the observations. However, for a conical basin ($m = 1$), the same mode ($k = 1$) has a natural frequency $\omega = f/5$. At 43° this gives a period of 88 h which is surprisingly close to that observed. This demonstrates the sensitivity of the natural period or frequency to bathymetric profile, at least for the gravest, non-steady vortex mode ($k = 1$).

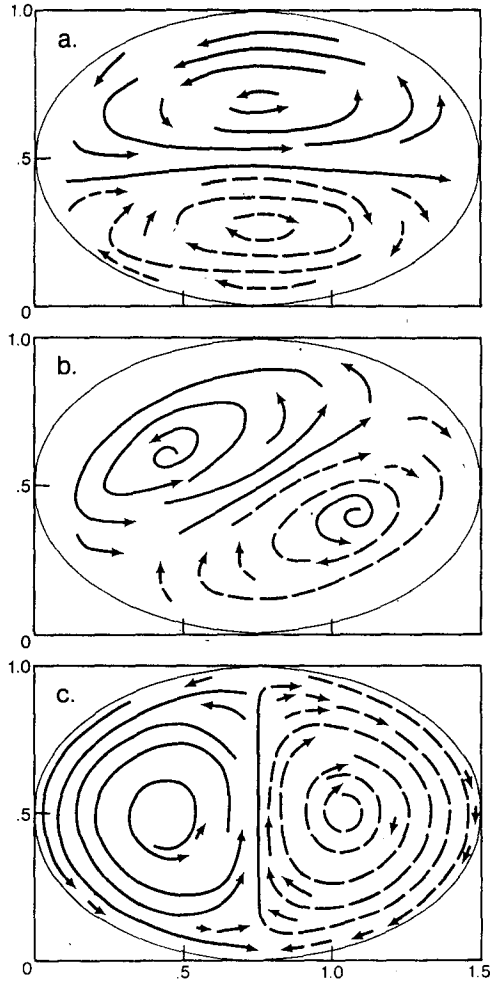

FIG. 12. Schematic streamline pattern of the two-cell vortex mode: (a) at $t = 0$, (b) at t = one-eighth period, and (c) at t = one-fourth period. Intersection of the nodal line of ψ with the boundary at different times shows the variable angular speed of propagation.

In the limit of large k, for fixed shape parameter m, Eq. (6) shows that $\omega \rightarrow f/3$. This is consistent with the maximum frequency of the quasi-geostrophic vortex modes given by Reid (1958) and others for the case of a shelf of constant slope with shoreline $h = 0$. In fact, for large k, Eq. (7) shows that the bulk of the kinetic energy of the vortex modes for the basin is confined to a narrow region of order $\Delta r = b/k$ near shore, as in the case of shelf wave theory. This correspondence with the boundary-trapped shelf wave theory applies even in a qualitative sense for modes $k = 2, 3$, etc. since the velocity for these modes vanishes at the basin center. However, the gravest mode $k = 1$ is unique in that it has a magnitude of velocity at the basin center which is comparable to the amplitude of V_ϕ at shore (in the ratio 1:2 m). For the conical basin this ratio is 0.5 while for the paraboloidal basin the ratio is only 0.25. The observed current magnitudes shown in Fig. 10 tend to favor the parameterization $m = 1$, which is consistent with the agreement of observed and calculated period using this parameterization.

The above estimates apply strictly to bathymetry with axial symmetry. The actual southern basin of Lake Michigan is more nearly elliptical with a ratio of major to minor axis of ~1.5. Ball (1965) gives solutions for the vortex modes in a basin with elliptic paraboloidal bathymetry given by

$$h = H(1 - \alpha x^2 - \beta y^2), \tag{10}$$

of which the circular basin is a special case when $\alpha = \beta = 1/b^2$. For the $k = 1$ mode, the natural frequency is

$$\omega = f\left(\frac{1 - \theta^2}{49 - 9\theta^2}\right)^{1/2}, \tag{11}$$

where

$$\theta = (\beta - \alpha)/(\beta + \alpha)$$

which reduces to $\omega = f/7$ when $\alpha = \beta$. For the ratio of major to minor axis mentioned earlier, this yields a natural frequency which is only ~6% smaller than that for the paraboloidal circular basin. The effect of the ellipticity, therefore, is much less than the difference due to change of bathymetry from paraboloidal to cone-shape.

The $k = 1$ circulational mode based on Ball's analysis is illustrated in Fig. 12. This clearly shows the two-cell structure of circulation and the cyclonic propagation of these cells. It is the only mode which is consistent with the behavior of the observed currents (counterclockwise rotation of the current vector near the basin center and clockwise rotation near the boundaries). The next higher azimuthal mode ($k = 2$) from Ball's model, as in the circular basin, gives a stagnation point for velocity at the basin center. This clearly does not fit the kinematic data, even though the natural period (93 h) for the elliptic paraboloidal basin for $k = 2$ is close to the observed period. Further evidence for the matching of the $k = 1$ mode with the observational data is provided by the phase relations for the northward components of velocity at stations 2, 3, 6 and 8 (Table 1). If we take the phase as zero at station 2, then there exists a progressive lag of 38, 74 and 135° at stations 3, 6 and 8. Taking the deepest point in the basin as the origin, the azimuths of these stations relative to station 2 are 34, 72 and 106°. If the southern basin were circular, then for the $k = 1$ mode the phases and azimuths relative to station 2 should be the same. The differences can be attributed to the more nearly elliptical shape, where Fig. 12 indicates a dependence of the angular velocity of the nodal line of streamfunction on azimuth.

5. Discussion

Certainly the pertinence of vortex modes in the Great Lakes has been recognized in previous work. One of the points we wish to emphasize as a result of this study is that, in order to properly deal with the gravest modes of this class of disturbance, one must treat the phenomena in a basin-wide sense. While the use of relations borrowed from topographic shelf wave models may work reasonably well near the coast for the higher azimuthal modes as in Csanady (1976), they are not valid for the gravest modes.

Our example computations in the previous section show that the frequency of such modes is sensitive to the form of the bathymetry. This confirms a similar finding by Rao and Schwab (1976), who also pointed out that the results of analyses of the natural modes is also sensitive to the computational method, when numerical methods are invoked. For the southern Lake Michigan basin, the parameterizations employed in order to estimate the natural period are clearly gross approximations of the real topography. The inverted cone-shaped basin gave the closest agreement with the observed energetic sub-inertial frequency. However, the paraboloidal shape seems closer to reality. If one considers the evidence for a mean cyclonic circulation in the basin then the period estimate for such a basin could be brought closer in line with the observed by taking into account the Doppler shift produced by the mean circulation.

In summary, we are convinced that the observed low-frequency resonant oscillatory phenomenon in southern Lake Michigan is the gravest second-class (vortex) mode in the lake basin. The gravest vortex modes may be observable features in other Great Lakes basins although, in most, sufficient data are not available for comparison; e.g., Marmorino (1979) found evidence of coherence at periods of 4 or 5 days in current recordings about the perimeter of Lake Ontario and Bennett and Saylor (1974) reported spectral kinetic energy peaks and coherences at slightly longer periods (higher rotational wave modes) in the same lake. Further observational studies will eventually provide these data and analytical studies must address the role of atmospheric forcing in generating and maintaining such vortex modes.

Acknowledgments. We gratefully acknowledge the contributions made by John L. Grumblatt and Gerald S. Miller in the preparation of data used in this report. D. B. Rao and the other reviewers also contributed valuable suggestions.

REFERENCES

Ball, F. K., 1965: Second-class motions of a shallow liquid. *J. Fluid Mech.*, **23**, 545–561.

Beardsley, R. C., W. Boicourt, L. C. Huff and J. Scott, 1977: CMICE 76: A current meter intercomparison experiment conducted off Long Island in February–March 1976. Tech. Rep. 77-62, WHOI, 123 pp. (unpublished manuscript).

Bennett, E. B., and J. H. Saylor, 1974: IFYGL water movement program: A post field work review. *Proc. IFYGL Symp., 55th Annual Meeting*, Amer. Geophys. Union, 102–127. [Published by NOAA, Dept. of Commerce, Rockville, Md.]

Birchfield, G. E., and B. P. Hickie, 1977: The time-dependent response of a circular basin of variable depth to a wind stress. *J. Phys. Oceanogr.*, **7**, 691–701.

Csanady, G. T., 1976: Topographic waves in Lake Ontario. *J. Phys. Oceanogr.*, **6**, 93–103.

——, and J. T. Scott, 1974: Baroclinic coastal jets in Lake Ontario during IFYGL. *J. Phys. Oceanogr.*, **4**, 524–541.

Gonella, J., 1972: A rotary-component method for analyzing meteorological and oceanographic time-series. *Deep-Sea Res.*, **19**, 833–846.

Hamblin, P. F., 1972: Some free oscillations of a rotating natural basin. Ph.D. thesis, University of Washington, 97 pp.

Huang, J. C. K., 1972: The thermal bar. *Geophys. Fluid Dyn.*, **3**, 1–25.

Lamb, H., 1932: *Hydrodynamics*. Dover, 730 pp.

Marmorino, G. O., 1979: Low-frequency current fluctuations in Lake Ontario, winter 1972–73. *J. Geophys. Res.*, **84**, 1206–1214.

Monahan, E. C., and P. C. Pilgrim, 1975: Coastwise currents in the vicinity of Chicago, and currents elsewhere in southern Lake Michigan. Tech. Rep., Dept. Atmos. Oceanic Sci., the University of Michigan, Ann Arbor, Mich. (unpublished manuscript).

Mortimer, C. H., 1963: Frontiers in physical limnology with particular reference to long waves in rotating basins. *Proc. 5th Conf. Great Lakes Res.*, Publ. No. 10, Great Lakes Res. Div., the University of Michigan, 9–42.

Rao, D. B., and D. J. Schwab, 1976: Two-dimensional normal modes in arbitrary enclosed basins on a rotating earth: Application to Lakes Ontario and Superior. *Phil. Trans. Roy. Soc. London*, **A281**, 63–96.

Reid, R. O., 1958: Effects of Coriolis force on edge waves. (I) Investigation of the normal modes. *J. Mar. Res.*, **16**, 109–144.

Simons, T. J., 1974: Verification of numerical models of Lake Ontario: Part I. Circulation in spring and early summer. *J. Phys. Oceanogr.*, **4**, 507–523.